2024

Establishing the consequences of NOTCH1 modulation, by small molecule inhibitors, on epithelium growth and differentiation

BOSTON UNIVERSITY

ARAM V. CHOBANIAN & EDWARD AVEDISIAN SCHOOL OF MEDICINE

Thesis

ESTABLISHING THE CONSEQUENCES OF NOTCH1 MODULATION, BY SMALL MOLECULE INHIBITORS, ON EPITHELIUM GROWTH AND DIFFERENTIATION

by

CAILYN J. KIRKALDY

B.S., Appalachian State University, 2021

Submitted in partial fulfillment of the

requirements for the degree of

Master of Science

2024

Approved by

First Reader ____
Sarah Mazzilli, Ph.D.
Assistant Professor of Medicine

Second Reader ____
Elizabeth Duffy, M.A.
Associate Professor of Pathology and Laboratory Medicine

Third Reader ____
Roxana Pfefferkorn, Ph.D.
Postdoctoral Fellow

DEDICATION

I would like to dedicate this work to the most amazing group of people anyone could ever have the pleasure of knowing – my friends and family. All of you, near and far, are the reason that I get up every day and do my best to make a positive impact on this world. I love you so much.

ACKNOWLEDGMENTS

I would first like to acknowledge the folks who really made this thesis possible. My deepest thanks are extended to Dr. Sarah Mazzilli, who so kindly welcomed me into the section of Computational Biomedicine and allowed me to grow and develop as a scientist. I have learned so much from Dr. Mazzilli's mentorship, and for that I will always be grateful. I would also like to thank Dr. Roxana Pfefferkorn and Emily Green, who trained me and helped me in countless ways both professionally and personally. These two magnificent women were shoulders to cry on (literally), friends, and the most amazing teachers a girl could ask for. It's also imperative that I shout out Elizabeth Duffy, who not only gave me the opportunity to learn and grow at Boston University, but pulled me back from many a spiral. I would have actually gone crazy without you Liz, so thank you for reminding me that I am capable and would be a-okay!

Finally, I would be remiss if I failed to acknowledge all of the educators who helped bring me to this place in my life. I always loved school growing up, and part of that is because of the amazing teachers and professors who raised me. Special thanks to Dr. Zodiac Webster and Dr. Nicholas Shaw – thank you for teaching me what it means to think critically and work like a scientist, as well as for supporting me well after I've left your classes and laboratories.

From the bottom of my heart, thank you all!

ESTABLISHING THE CONSEQUENCES OF NOTCH1 MODULATION, BY SMALL MOLECULE INHIBITORS, ON BRONCHIAL EPITHELIUM GROWTH AND DIFFERENTIATION.

CAILYN J. KIRKALDY

ABSTRACT

Lung cancer is the third most diagnosed and deadly cancer in the United States annually, with lung squamous cell carcinoma (LUSC) being heavily associated with smokers. Prognosis declines with the stage of lung cancer at diagnosis, with stage IA patients having a 50% 5-year survival rate and patients diagnosed with stage IIIA lung cancer having only a 19% 5-year survival. While diagnosis and screening protocols have improved survival rates and our understanding of cancer through projects like The Cancer Genome Atlas, focus has shifted toward detecting lung cancer before it becomes established. Premalignant lesions arise before becoming invasive cancer, and can either regress to normal tissue or progress through histological grades before becoming carcinoma *in situ* and established lung carcinoma.

Previous studies focused on LUSC premalignancy within the section of Computational Biomedicine at Boston University's Chobanian and Avedisian School of Medicine have used genomic and transcriptomic sequencing on patient biopsies to identify common mutations and subsequent transcriptomic changes found in bronchial premalignant lesions. In 41% of the biopsies taken from patients, there are mutations in the *NOTCH1* gene. NOTCH is a membrane protein used for cell signaling, and is particularly important for tissue development and injury repair. The NOTCH pathway

maintains resident stem cell populations, prompting them to regenerate and differentiate when necessary. The role of NOTCH in tumorigenesis is complex; in some cancers NOTCH mutations are a driver of cancer and in others a tumor suppressor. In this thesis, small molecule inhibitors were used to inhibit NOTCH1 in order to understand the role of NOTCH1 modulation in the bronchial epithelium.

Three aims were devised to study the role of NOTCH1 *in vitro* using bronchial epithelium cell lines. The first aim sought to establish the sensitivity and effectiveness of small molecule NOTCH1 inhibitors in immortalized bronchial epithelial cells to establish the dosages used for future experimentation. Using qRT-PCR, it was observed that 5 uM doses of small molecule inhibitors effectively inhibit NOTCH1 in immortalized bronchial epithelial cells. The second aim focused on the consequences of NOTCH1 modulation on cell growth which was inhibited by the 5 uM dose of small molecule inhibitors NADI-351 and DAPT, but not Crenigacestat. Finally, primary bronchial epithelial cells were cultured at the air-liquid interface to stimulate differentiation and observe change in cell populations when NOTCH1 was inhibited. Primary bronchial epithelial cells grown at the air-liquid interface with 1 uM treatments had noticeable differences in tissue size and cell differentiation in the two γ-secretase inhibitors, Crenigacestat and DAPT.

TABLE OF CONTENTS

LIST OF TABLES

LIST OF FIGURES

LIST OF ABBREVIATIONS

ALI .... Air-liquid interface

ATP .... Adenosine triphosphate

Ct .... Cycle threshold

CT .... Computed tomography

DDi .... Distilled deionized

H+E .... Hematoxylin and eosin

HBEC .... Human bronchial epithelial cell

HBEC3-KT .... Immortalized human bronchial epithelial cell

IF .... Immunofluorescence

IMC .... Image mass cytometry

Lof .... Loss of function

LUAD .... Lung adenocarcinoma

LUSC .... Lung squamous cell carcinoma

MTT .... 3-(4,5-dimethylthiazol-2-yl)-2,5-diphenyltetrazolium bromide

NICD .... NOTCH intracellular domain

NSCLC .... Non-small cell lung cancer

PBS-T .... Phosphate buffered saline with tween

PCGA .... Pre-Cancer Genome Atlas

PET .... Positron emission tomography

pHBEC .... Primary human bronchial epithelial cell

PML .... Premalignant Lesion

R^2 .... Correlation Coefficient

SMI .... Small Molecule Inhibitor

TCGA .... The Cancer Genome Atlas

INTRODUCTION

Lung Cancer

In 2023 the National Cancer Institute reported that lung and bronchial cancer is the third most diagnosed cancer in the United States, and the most deadly (Figure 1)[1]. There are two types of lung cancer, small cell lung cancer and non-small cell lung cancer (NSCLC), with NSCLC making up nearly 80% of lung cancers[2]. NSCLC can be broken up even further into three subtypes: lung adenocarcinoma (LUAD), lung squamous cell carcinoma (LUSC), and large cell carcinoma. LUSC is mostly associated with smokers, and occurs in the airway and central lung[2–4]. Previous studies have shown that while LUAD is more prevalent, patients with LUSC have a poorer overall survival[5,6]. However, this could be a reflection of accompanying comorbidities found in patients with LUSC such as higher alcohol consumption, vascular diseases, and other pulmonary complications.

Cancer Statistics 2023

Estimated Cancer Deaths in the US in 2023

Male		
Lung & bronchus	67,160	21%
Prostate	34,700	11%
Colon & rectum	28,470	9%
Pancreas	26,620	8%
Liver & intrahepatic bile duct	19,000	6%
Leukemia	13,900	4%
Esophagus	12,920	4%
Urinary bladder	12,160	4%
Non-Hodgkin lymphoma	11,780	4%
Brain & other nervous system	11,020	3%
All sites	**322,080**	

Female		
Lung & bronchus	59,910	21%
Breast	43,170	15%
Colon & rectum	24,080	8%
Pancreas	23,930	8%
Ovary	13,270	5%
Uterine corpus	13,030	5%
Liver & intrahepatic bile duct	10,380	4%
Leukemia	9,810	3%
Non-Hodgkin lymphoma	8,400	3%
Brain & other nervous system	7,970	3%
All sites	**287,740**	

Figure 1. Estimated Cancer Deaths in the United States in 2023, by sex. American Cancer Society. Cancer Fast Facts & Figures 2023. Atlanta: American Cancer Society, Inc. 2023.

Current methods for diagnosing LUSC first employ imaging like, computed tomography (CT) scans and/or positron emission tomography (PET), which allow physicians to image the airways, lungs and surrounding tissues and determine if there are any abnormal areas[7]. In the event that a patient has a notable result from imaging, the physician may collect lung and or lymph node samples to confirm the presence and stage of cancer. Sample collection can be performed in a variety of ways, including biopsy taken via bronchoscopy, collecting sputum, and even airway brushings[7–9]. Imaging, along with laboratory results, are then used to stage the cancer based on the size, if the cancer has infiltrated surrounding lymph nodes, and if metastasis has occurred[10]. The stage of a cancer at diagnosis can be an indicator of the patient's treatment and five-year survival, which is why it is so important to have clear tumor grading systems. Lung cancer patients with a clinical stage IA have a 50% five-year survival, whereas patients with a clinical stage IIIA only have a 19% five-year survival[11]. The difference in five-year survival between stages emphasizes a need for better screenings and diagnostics, so that cancers can be detected before they reach these higher stages.

Improvements in early detection of lung cancer have focused on reducing mortality with the implementation of lung cancer screening guidelines, driving the field to identify key biomarkers and develop intervention strategies for early stage diagnosis. Accomplishing those goals, however, requires an understanding of the natural progression of lung lesions, from premalignant lesions to established tumors. Consortia efforts such as The Cancer Genome Atlas (TCGA) used molecular and genomic tools to profile 33 cancer types, including data on NSCLC (LUAD and LUSC), to better understand established tumors and the tumor microenvironment[12,13]. As data from TCGA was compiled, researchers identified the most commonly mutated genes and pathways as biomarkers and therapeutic targets for cancer[12]. Improvements to diagnostic testing through biomarker discovery and cutting edge diagnostic tools enhance patient care by cutting down on uncertainties, providing quicker results from the laboratory, and cutting out unnecessary or invasive procedures. However, improvements to diagnostic testing and screening can only be used in the context of existing cancer, meaning these cancers have already become established and are putting the patients at risk of progression to higher stages and poorer prognosis.

Lung Squamous Premalignant Lesions

Premalignant lesions (PMLs) are precancerous patches of tissue that have morphological changes, but have not invaded the basement membrane or surrounding tissue[14]. When an individual inhales an irritant, such as cigarette smoke or environmental irritants, the airway walls can become injured. Repeated injury due to occupational exposures or smoking can cause sustained injuries which form lesions. Squamous PMLs largely progress in a stepwise manner from hyperplasia, metaplasia, dysplasia of varying severity, and carcinoma *in situ*, before becoming LUSC (Figure 2)[15–17]. However, not all lesions progress to become cancer, as most spontaneously regress to normal tissue[17].

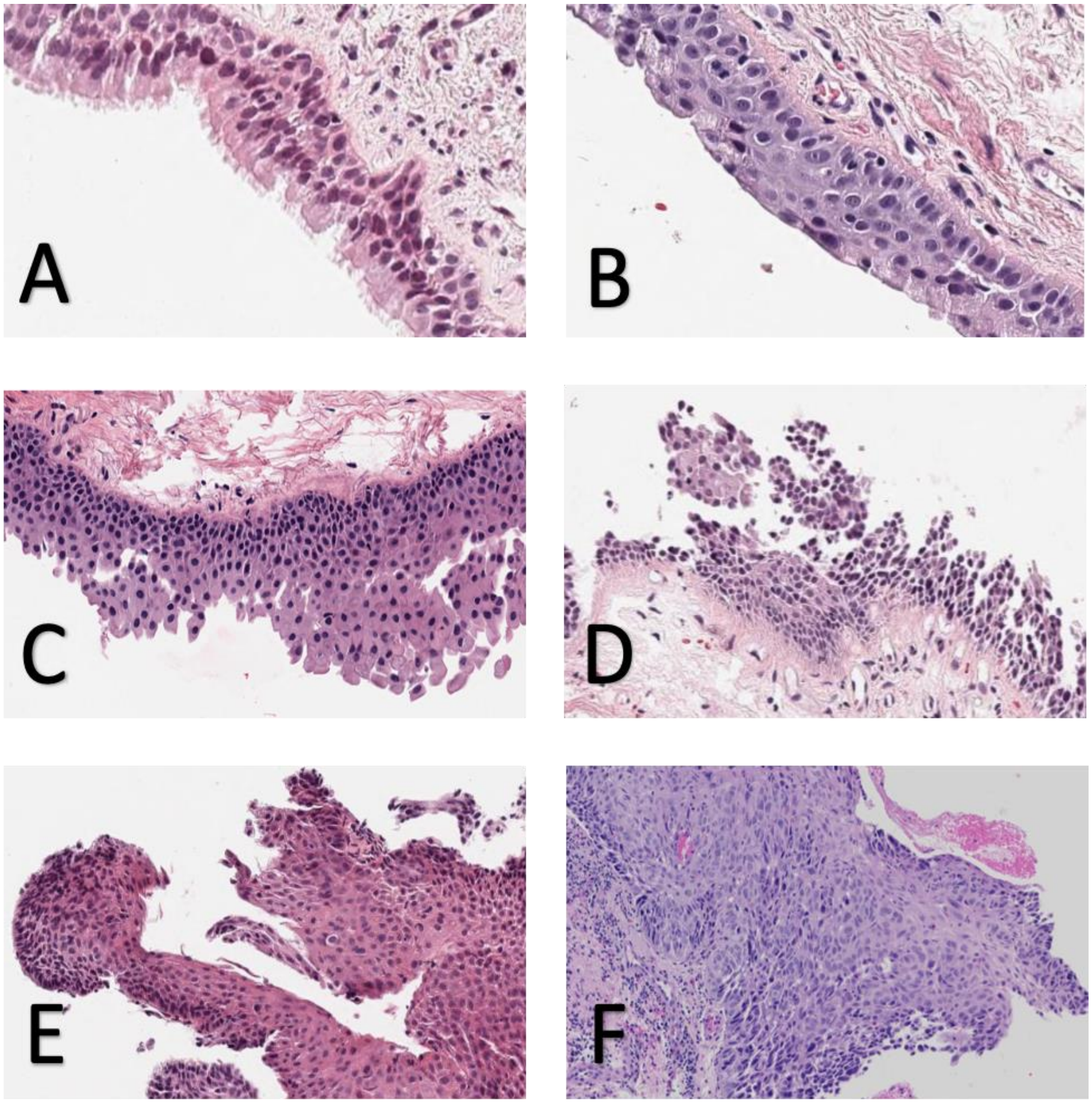

Figure 2. Progression of lesions from normal epithelial tissue to carcinoma in situ. (a) Normal tissue, (b) squamous metaplasia, (c) mild dysplasia, (d) moderate dysplasia, (e) severe dysplasia, and (f) carcinoma in situ. Images provided by Roswell Park in collaboration with the National Caner Institute’s Pre-Cancer Genome Atlas Project.

In the previous decade, the focus of cancer research has shifted from just improving established cancer diagnosis and treatment to studying cancer before it becomes established and is identified as precancerous lesions. Understanding the mechanisms of progression of PML to LUSC, or regression to normal tissue, is paramount to interrupting the development of cancer and providing patients with tailored, lesion-specific treatment options. Our group and others have contributed to the establishment of the Lung Pre-Cancer Genome Atlases (PCGAs) which aim to expand our understanding of the preinvasive lesion and its environment on a molecular and cellular level[18]. In the same ways that TCGA worked to uncover the characteristics and hallmarks of advanced cancers, PCGA has begun to unravel the way that PML develop and progress or regress. The biggest call to action put forth by the researchers behind PCGA was the need for longitudinal studies of genetic profiles and microenvironments of these PML as they evolve into LUSC or regress to normal tissue[18]. By understanding the progression of these lesions from injury to malignancy, as well as their influence on the surrounding environment or relationship with the immune system, biomarkers of progressive disease and potential treatments can be identified.

One of the first steps to achieving the goals set by PCGA is to identify PML in patient airways. Our group previously identified a 200-gene transcriptional biomarker for detecting PML in patients by studying the normal appearing airway, which uncovered an upregulation in genes involved in energy production in patients with PML[19]. Following this, our group profiled bronchial brushings and biopsies by RNA sequencing taken during routine screening from high-risk patients, aimed to characterize the molecular differences between PML. This study identified four distinct molecular subtypes of PML - proliferative, inflammatory, secretory, and normal-like. Of the four profiled subtypes, the *Proliferative* subtype was most closely associated with dysplastic and persistent characteristics and therefore the most likely to develop into LUSC[20]. While the mechanisms underlying these four distinct classifications are not fully understood, analysis of the genetic expression of the *Proliferative* subtype does point towards an upregulation of metabolic and cell cycle pathways in these lesions, and a lack of immune response due to a decrease in the expression of genes involved in immune signaling and antigen presentation in the progressive *Proliferative* lesions[20]. This project not only furthered our understanding of the hallmarks of progressive lesions, but it also encouraged further research into the mechanisms behind PML progression to LUSC.

Ongoing research has focused largely on filling in those mechanistic gaps. Once again using samples acquired during bronchoscopy of high-risk patients, our group performed whole exome and targeted DNA sequencing to elucidate the role of genomic alterations in PML progression, revealing that *NOTCH1* was the most frequently (up 41% of lesions) mutated gene in PML with mutations primarily resulting in loss of function (lof) mutation. Importantly, $NOTCH1^{lof}$ is more frequent in PMLs than in advanced LUSC from TCGA, suggesting that this is an important characteristic of the precancerous environment (Figure 3)[21]. To establish potential biologic consequences of $NOTCH1^{lof}$ analysis of transcriptomic and Imaging Mass Cytometry (IMC) proteomic data revealed that the *NOTCH1* mutation alters cell phenotypes and potential differentiation trajectories found in the lesion, promoting a secretory intermediate called a peri-goblet cell, rather than the ciliated cells that typically dominate the airway architecture[21,22]. Discoveries like peri-goblet cells, which had previously been unidentified[23], in the context of *NOTCH1[lof]* encourages a need for further mechanistic study into how *NOTCH1* modulation is involved in the premalignant environment and how it relates to the determination of cell fates.

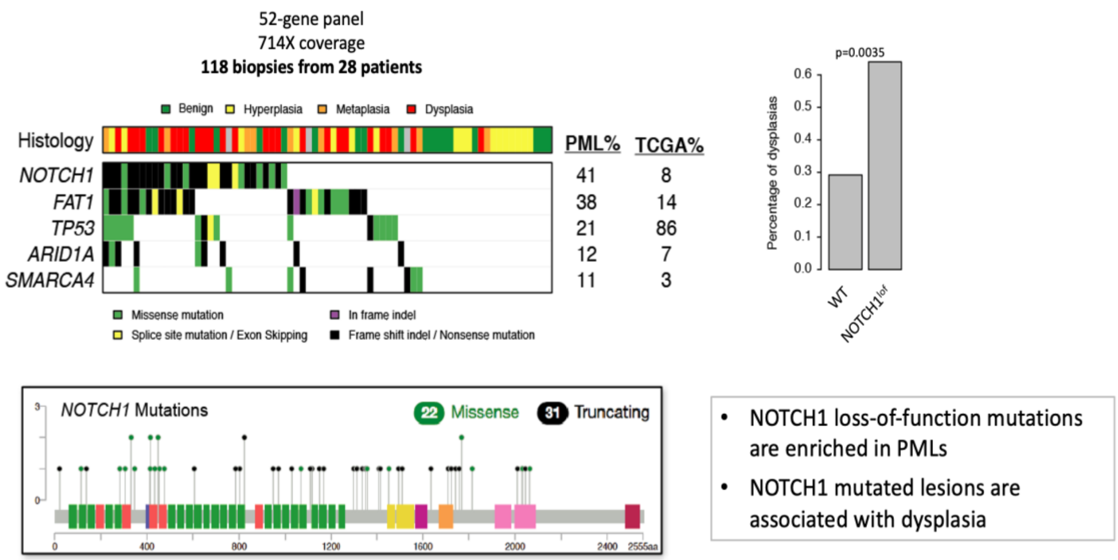

Figure 3. Sequencing results and analysis provided by Roxana Pfefferkorn. Performed by Diyva Venkatraman and Joshua Campbell.

The NOTCH *Pathway*

The NOTCH pathway is a complex pathway involved in the differentiation of cells, and the maintenance of stem cell populations[24]. Functionally, there are four NOTCH transmembrane receptors, and when bound to ligands found on neighboring cells these receptors are cleaved twice by cell-surface proteases such as γ-secretase and

ADAM/TACE metalloproteases[24,25]. This separates the NOTCH extracellular domain from the NOTCH intracellular domain (NICD), the latter of which moves to the nucleus and binds to a series of proteins to form the CSL protein complex which acts as a transcription factor (Figure 4)[25].

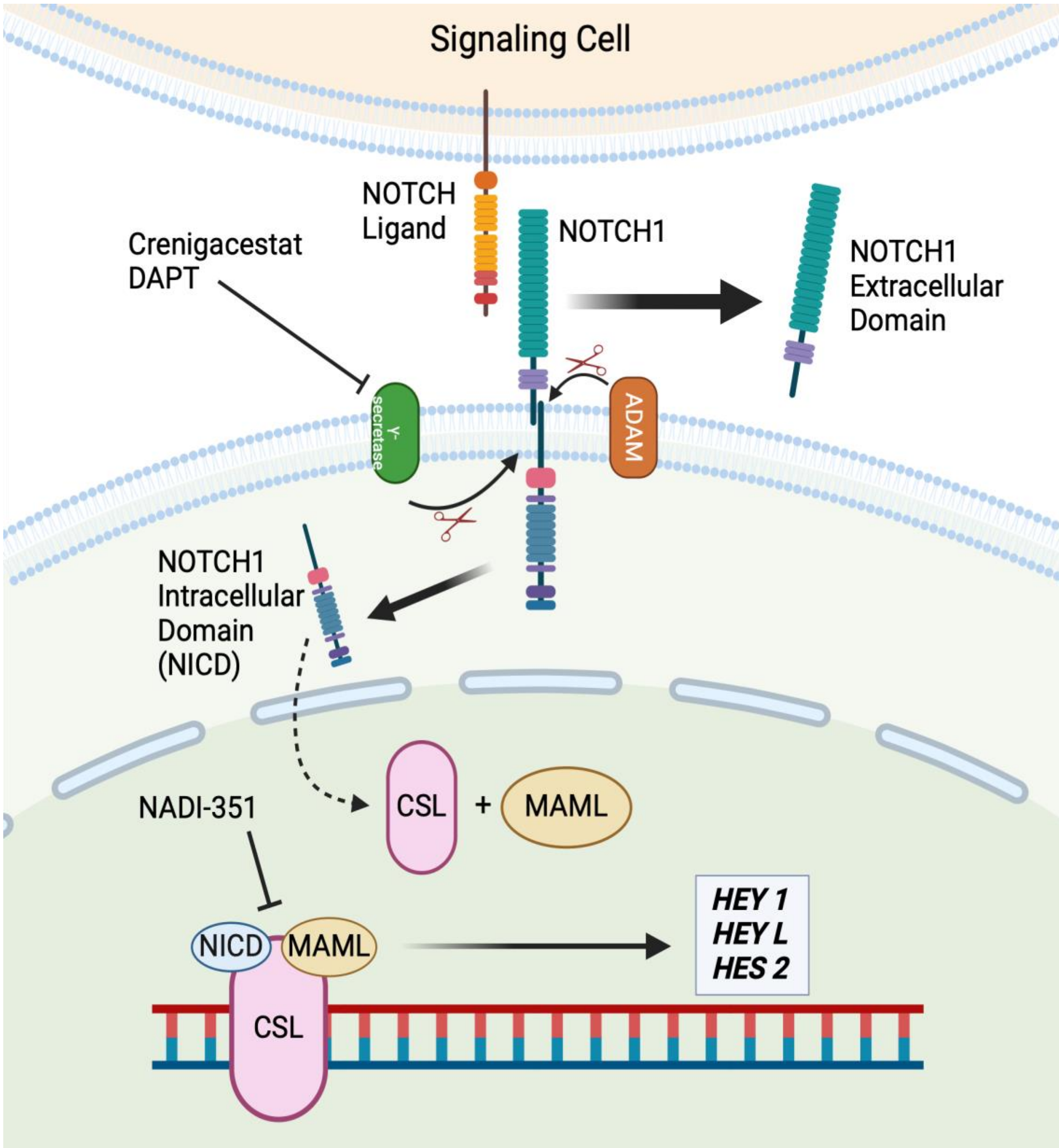

Figure 4. The Notch pathway and the inhibitors that will be used in this study. Created with Biorender.com.

Previous work by Rock, et al. revealed that Notch loss-of-function mutations in mouse airway models hindered basal cell differentiation, but did not prevent the basal cells from progressing to an early progenitor of secretory and ciliated cells, and that at homeostasis Notch signaling is not commonly active, but becomes active after injury[26]. This is particularly interesting in the context of lung cancer, since LUSC most commonly occurs in smokers[27]. As we know, smoking causes injury to the airways through repeated exposure to irritants and carcinogens. Typical airway tissue consists mainly of ciliated cells and secretory cells like goblet and club cells, which stem primarily from basal cell populations. When the NOTCH pathway is activated, e.g. in the event of an injury, basal cells are prompted to differentiate and higher levels of NOTCH typically promote secretory differentiation whereas lower levels of NOTCH promotes the differentiation of ciliated cells (Figure 5)[26,28]. Therefore we hypothesize that $NOTCH^{lof}$ could indeed be playing an important role in the precancerous environment, since mutations in *NOTCH1* could be preventing normal injury repair and leaving basal cells in a state of partial-differentiation similar to peri-goblet cells.

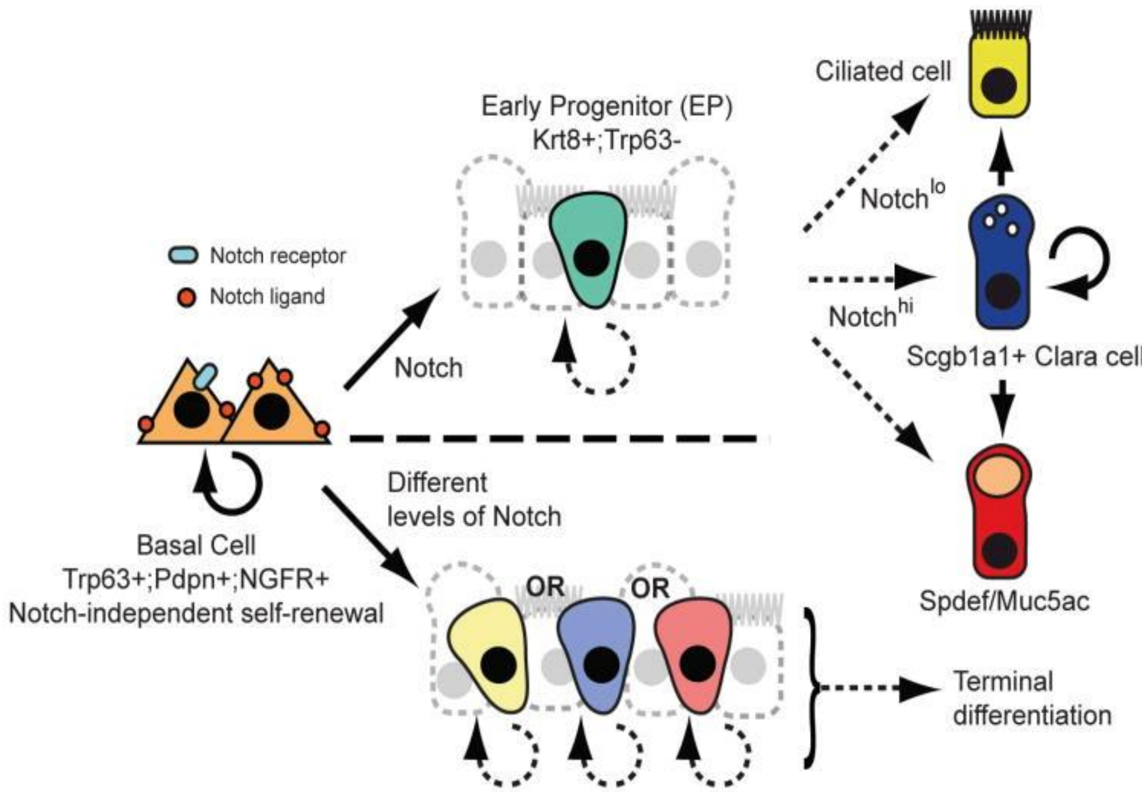

Figure 5. Proposed process of NOTCH-directed cell differentiation from basal cell to mature adult airway cell. Rock, J. R. et al., *Cell Stem Cell* (2011).

The effect of NOTCH modulation on cell growth and proliferation is inconsistent across studies. A study from 2009 suggests that *NOTCH* gain of function mutations are a driver of NSCLC and that NOTCH-dependent cells could be treated with γ-secretase inhibitors, including DAPT[29]. Another study presents the opposite, that *Notch1* overexpression in mice inhibited cell growth in adenocarcinoma cell lines by inducing cell cycle arest[30]. This suggests that the role NOTCH plays in tumorigenesis and cell growth is largely context dependent, and is likely influenced by extrinsic factors within the microenvironment. More work is needed to fully understand how the inhibition of NOTCH in airway epithelial cells affects growth and differentiation.

The idea that mutations found in the Notch pathway can lead to cancer is not novel. While each organ system may make use of different NOTCH receptors or accessory molecules, the pathway is largely conserved across different species[31]. The NOTCH pathway is similarly implicated in diseases characterized by changes to cell differentiation; for example, NOTCH alterations have been linked to Barrett's esophagus, a disease where normally stratified squamous tissue of the esophagus transforms into metaplastic columnar epithelia[32]. A study published by Kunze et al. in 2021 explored the relationship between the kinase Dclk1 and Barrett's esophagus in mice models that had either an activation of the NOTCH pathway, or an inhibition of the NOTCH pathway by removing the receptor NOTCH2. This study showed that NOTCH activation in Dclk1-positive cells showed a progression of Barrett's esophagus, rather than the delay in progression found in the Notch-inhibited mice[32]. Once again this modulation of the NOTCH pathway seems to impact the architecture of tissues in the context of disease. Another instance of changes in NOTCH expression in the gastrointestinal tract can be found in the intestines. A 2005 study reported that NOTCH inhibition via γ-secretase inhibitor DBZ led to an increase in goblet cells in intestinal crypts and adenomas[33]. This study further supports our observation that NOTCH-mutated PML exhibit a loss of ciliated cell populations in favor of secretory cells. The focus of this thesis work is to further explore *NOTCH1* and its role in bronchial epithelium by establishing the consequences of NOTCH1 inhibition in primary and immortalized human bronchial epithelial cells (HBEC).

Thesis Aims

To better understand how the modulation of the Notch pathway affects bronchial epithelia, this thesis test the consequences of inhibiting NOTCH1 in human airway epithelium. To inhibit the NOTCH pathway, three small molecule inhibitor (SMI) drugs will be used. Two of the inhibitory drugs used in this research are the γ-secretase inhibitors DAPT and Crenigacestat. These drugs prevent the cleavage of NOTCH1, which halts the pathway before NICD can separate and move to the nucleus[34,35]. The final small molecule inhibitor, NADI-351, is a novel drug that specifically targets NOTCH1 by preventing the formation of the CSL transcription complex[36].

Aim 1. Establish the dose of SMI to employ in immortalized bronchial epithelial cells, HBEC3-KT, and to measure sensitivity and specificity of NOTCH inhibition. We will demonstrate that the inhibition of NOTCH1 affects the expression of genes controlled by the NICD/CSL complex. NOTCH1 will be inhibited by small molecule drug delivery in immortalized human bronchial epithelial cells (HBEC3-KT) cultured in monolayer for the duration of one week. Following treatment, qRT-PCR will be used to measure the expression of genes downstream of the NOTCH pathway. It is our hypothesis that the small molecule drugs we have chosen will effectively inhibit the NOTCH pathway. We expect to see a decrease in the expression of target genes downstream of the NOTCH pathway.

Aim 2. Test the effect of NOTCH1 inhibition on the growth of the HBEC3-KT. Immortalized HBEC3-KT cells will be grown in monolayer cultures for the duration of one week, with cell counts being taken at day two, day five, and day seven. It is our hypothesis that the inhibition of NOTCH1 will decrease the number of immortalized epithelial cells.

Aim 3. Observe the effect of NOTCH1 inhibition on basal cell differentiation in primary epithelial cells. Finally, using the same SMI treatment, primary HBEC will be grown at air-liquid interface (ALI) to establish the effects of NOTCH1 inhibition on the differentiation of bronchial epithelium. At the conclusion of this ALI study, cells grown on transwell membranes will be harvested for further qRT-PCR analysis, and imaging by hematoxylin and eosin (H+E) and immunofluorescence (IF) staining. We hypothesize that the inhibition of the NOTCH1 pathway will modify the differentiation of our primary HBEC tissues. We expect that the cultures treated with our small molecule drugs will have shifted cell populations.

Using immortalized and primary HBECs we modeled the effects of NOTCH1 pathway inhibition through SMI. We observe that 5 uM doses of SMI were effective for inhibiting NOTCH1 in immortalized HBECs, but when primary cells are grown at the ALI a 5 uM dose displays some toxicity. Furthermore, immortalized HBEC growth was inhibited by the 5 uM dose of NADI-351 and DAPT, but not Crenigacestat. Finally, when primary HBECs were grown at the ALI with 1 uM SMI treatments, there were noticeable differences in tissue size and cell differentiation in Crenigacestat- and DAPT-treated cultures. While these experiments are great pilots for informing future studies, no significant conclusions could be drawn. However, these results do suggest that the inhibition of the NOTCH1 pathway in bronchial epithelial cells does affect growth and differentiation.

METHODS

Materials

Table 1. Cell Lines and Small Molecule Inhibitors

Item	**Supplier**	**Catalog Number**
Normal human bronchial epithelial cells (NHBE)	Lonza	21TL076045 21TL019233 22TLL073038 22TL332333 23TL072012
HBEC3-KT cells	American Type Culture Collection (ATCC)	CRL-4051
NADI-351	ProbeChem	PC-72454
Crenigacestat (LY3039478)	Selleckchem	S7169
DAPT (GSI-IX, LY-374973)	Selleckchem	S2215

Table 2. Cell Culture Reagents

Item	**Supplier**	**Catalog Number**
PneumaCult-Ex Plus Basal Media	STEMCELL Technologies	05041
PneumaCult-Ex Plus 50x Supplement	STEMCELL Technologies	05042

PneumaCult-ALI Basal Media	STEMCELL Technologies	05002
PneumaCult-ALI 10x Supplement	STEMCELL Technologies	05003
PneumaCult-ALI Maintenance Supplement 100x	STEMCELL Technologies	05006
Penicillin-Streptomycin (100x)	Gibco	15140-122
Heparin Solution (0.2%)	STEMCELL Technologies	07980
Hydrocortisone (96 ug/mL)	STEMCELL Technologies	07925
Human collagen IV	Millipore Sigma	CC076

Table 3. qRT-PCR Analysis

Item	**Supplier**	**Catalog Number**
Trypsin-EDTA	Cell Applications, Inc.	070-100
QIAzol Lysis Reagent	QIAGEN	79306
Transcriptor First Strand cDNA Synthesis Kit	Roche	04896866001

SuperScript IV Single Cell/ Low-Input cDNA PreAmp Kit	Invitrogen by Thermo Fisher Scientific	11752048
TaqMan Fast Advanced Master Mix	Applied Biosystems by Thermo Fisher Scientific	4444557
TaqMan 20x PPIA Primer (Hs04194521_s1)	Applied Biosystems by Thermo Fisher Scientific	4331182
TaqMan 20x NOTCH1 Primer (Hs01062014_m1)	Applied Biosystems by Thermo Fisher Scientific	4453320
TaqMan 20x HEY1 Primer (Hs05047713_s1)	Applied Biosystems by Thermo Fisher Scientific	4453320
TaqMan 20x HEYL Primer (Hs00232718_m1)	Applied Biosystems by Thermo Fisher Scientific	4453320
TaqMan 20x HES2 Primer (Hs10121800_g1)	Applied Biosystems by Thermo Fisher Scientific	4448892
TaqMan 20x BCL2 Primer (Hs04986394_s1)	Applied Biosystems by Thermo Fisher Scientific	4453320
TaqMan 20x BAX Primer (Hs00180269_m1)	Applied Biosystems by Thermo Fisher Scientific	4453320
TaqMan 20x CASPASE-3 Primer (Hs00234387_m1)	Applied Biosystems by Thermo Fisher Scientific	4453320

Table 4. Immunofluorescence Staining

Item	**Supplier**	**Catalog Number**
Citrate Buffer, pH 6.0, 10x, Antigen Retriever	Sigma-Aldrich	C9999
SuperBlock Blocking buffer	Thermo Scientific	37515
Keratin 8 (TROMA-1-C) Rat Antibody	Developmental Studies Hybridoma Bank	n/a
CEACAM5 Mouse Antibody	ProMab Biotechnologies	30157
MUC5AC Rabbit Antibody	Abcam	ab198294
NOTCH1 Rabbit Antibody	Rockland Immunochemicals, Inc.	100-401-405
Donkey anti-Rat IgG, Alexa Fluor 594	Invitrogen by Thermo Fisher Scientific	A-21209
Goat anti-Mouse IgG, Alexa Fluor 488	Invitrogen by Thermo Fisher Scientific	A-11001
Donkey anti-Rabbit IgG, Alexa Fluor 647	Invitrogen by Thermo Fisher Scientific	A-31573

ProLong Gold antifade reagent with DAPI	Invitrogen by Thermo Fisher Scientific	P36931

Cell Culture

Data collected for this project was generated using human airway cell culture models. For the analysis of growth and to demonstrate the inhibition of NOTCH1, HBEC3-KT cells, which are hTERT-immortalized human bronchial epithelial cells, were expanded in PneumaCult-Ex Plus culture media supplemented with 1% Penicillin-Streptomycin, the manufacturer's provided PneumaCult-Ex Plus 50x Supplement, and 0.1% hydrocortisone. After expansion, the cells were collected with a trypsin-EDTA solution, and seeded at 100,000 cells into 12-well plates for treatment. Using the same supplemented PneumaCult-Ex Plus media, 1 uM, 5 uM, and 10 uM treatments were prepared for DAPT, Crenigacestat, and NADI-351. Control treatments of DMSO were also prepared using the supplemented PneumaCult-Ex Plus media in concentrations of 0.1%, 0.5%, and 1%. For the duration of these experiments, from expansion through treatment, cells were incubated at 37°C and 5% CO_2.

Treatment with Small Molecule inhibitors

To demonstrate the effect of small molecule inhibition on differentiation, primary normal human bronchial epithelial cells (pHBEC) were taken directly from liquid nitrogen storage and seeded at 22,500 cells per donor (21TL076045, and 21TL019233) in 6.5 mm transwells which had previously been coated with a 1:10 solution of 1 mg/mL human collagen IV in nuclease-free water and allowed to air dry, and then UV treated for 30 minutes before use. These cells were expanded in the supplemented PneumaCult-Ex Plus media, with media placed in the bottom well and in the suspended transwell. Once 100% confluence was reached, the top layer of media was removed (Figure 6), and the cells were treated with 5 uM small molecule inhibitor and 0.5% DMSO control in PneumaCult-ALI Medium supplemented with the manufacturer supplied PneumaCult-ALI 10x supplement, 1% manufacturer supplied PneumaCult-ALI Maintenance Supplement 100x, 1% Penicillin-Streptomycin, 0.2% heparin solution, and 0.5% hydrocortisone. We began to lose the 5 uM treated cells shortly after treatment, so they were collected early for RNA isolation. A separate set of pHBEC cells - three donors, seeded in equal amounts of 15,000 cells (22TLL073038, 22TL332333, 23TL072012) - were cultured with the same media and in the same incubation conditions, but were treated with 1 uM concentrations of the small molecule inhibitors and 0.1% DMSO control. These 1 uM treated cells were incubated in a 37°C incubator at 5% CO_2 for 27 days post-airlift before collecting for RNA isolation and slide preparation.

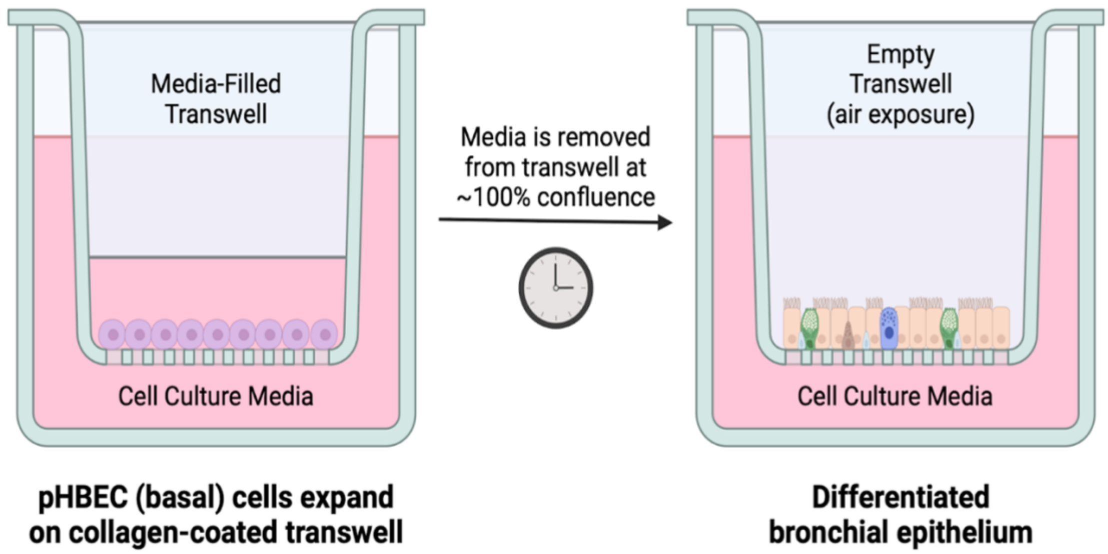

Figure 6. Cell culture diagram depicting the process of air lifting cells to stimulate primary HBEC cell differentiation. Created with Biorender.com.

Growth Analysis

Immortalized HBEC3-KT cells were cultured in PneumaCult-Ex Plus media supplemented with 5 uM concentrations of small molecule NOTCH1 inhibitors DAPT, Crenigacestat or NADI-351 as described above. The cells were cultured for one week, with wells being harvested on days two, five, and seven. Three wells were harvested on each day, and the cells were centrifuged to a pellet and then resuspended in 1 mL of media. Cell counts were taken using disposable cytometers (Cellometer Cell Counting Chambers, Nexcelom Bioscience, Lawrence, MA) and an automatic cell counter (Cellometer Auto 1000, Nexcelom Bioscience, Lawrence, MA).

RNA Isolation

Following the treatment period, cells were harvested and lysed for phenol-chloroform RNA extraction using 1 mL of Qiazol lysis reagent to which 250 uL chloroform was added. Centrifugation at 10,000 x g and 4°C for 15 minutes separated the aqueous from organic layers, allowing for the transfer of the aqueous layer to a clean tube where it is incubated overnight at 4°C with 100% ethanol to precipitate nucleic acids. Another centrifugation at 20,000 x g and 4°C pelleted any precipitated RNA. This pellet was then washed three times with 100% ethanol, 80% ethanol, and 100% ethanol respectively. After the final wash, the supernatant was removed and the pellet was allowed to air dry until the ethanol had evaporated. The remaining pellet of RNA was resuspended with 20 uL of nuclease-free water and measured using the NanoDrop spectrophotometer.

cDNA synthesis

RNA extracted through phenol-chloroform extraction was diluted 1 ug of RNA in 10 uL of nuclease-free water in a PCR tube. In a separate tube, a master mix was prepared using the Transcriptor First Strand cDNA synthesis kit. The master mix includes 4 uL of Transcriptor RT Reaction Buffer 5x, 2 uL of Deoxynucleotide Mix, 2 uL of Random Hexamer Primer, 1 uL of Anchored-oligo(dT)18 Primer, 0.50 uL of Protector RNase Inhibitor, and 0.50 uL of Transcriptor Reverse Transcriptase. The total volume of this master mix was 10 uL per reaction, which is added to each diluted RNA sample and mixed thoroughly. The assembled reaction mixture was then spun down and placed in a thermocycler where they are incubated at 25°C for 10 minutes, 55°C for 30 minutes, 85°C for 5 minutes, and then held at 4°C until stopped. Using the NanoDrop spectrophotometer, the absorbance at 280 nm was measured to infer cDNA concentration. For the cells grown at ALI, the SuperScript IV Single Cell/ Low-Input cDNA PreAmp kit was used to manufacturer's specifications. Using RNA isolated through phenol-chloroform extraction, 10 ng of RNA was diluted in the lysis and hybridization buffer.

qRT-PCR

qRT-PCR began by preparing a master mix comprised of 10 uL of TaqMan Fast Advanced Master Mix for qPCR, 7 uL of nuclease-free water, and 1 uL of 20x TaqMan Gene Expression Assay primer, per reaction well. The primers used for the purposes of this thesis work are shown in Table 3. In a separate tube, 1-100 ng of cDNA was diluted to 2 uL with nuclease-free water, per reaction well. In a 96-well plate, 18 uL of master mix and 2 uL of diluted cDNA was added to a well, mixing thoroughly. The 96-well plate was tightly sealed with a clear adhesive film. The plate was vortexed, the wells were gently flicked to pop bubbles, and the plate was briefly centrifuged to ensure all of the sample and master mix was at the base of the well. Finally, the 96-well plate was loaded onto the StepOnePlus Real-Time PCR instrument. The plate was incubated for one cycle by the instrument at 98°C for 10 seconds (denature), for 35 cycles at 98°C for one second, 55°C for five seconds, 72°C for 30 seconds (amplification), and for one cycle at

72°C for two minutes (final elongation). After the final elongation cycle, the StepOnePlus Real-Time PCR instrument held the 96-well plate at 4°C until stopped. Data collected from qRT-PCR was analyzed using $2^{-\Delta\Delta CT}$ PCR analysis. This type of analysis compares threshold cycles (Ct) between controls - usually a housekeeping gene such as the PPIA used here - and targets[37]. The $2^{-\Delta\Delta CT}$ values between replicates are averaged, and then plotted as bar charts, with their standard deviations as error bars.

Tissue Processing

ALI cultures were prepared for paraffin embedding by fixing them in 10% formalin for 30 minutes at room temperature, followed by 15 minute incubations in 50% ethanol, 70% ethanol, 80% ethanol, and 95% ethanol. The ALIs were then incubated in two consecutive 100% ethanol baths for 10 minutes a piece, followed by two more incubations in Slide Brite for another 10 minutes a piece. After dehydration the ALI transwells were placed in paraffin at 60°C for 10 minutes, followed by two more paraffin steps at 60°C for 15 minutes each. Finally, the membranes were cut out of the transwell and cut in half, with each half being placed perpendicularly within a mold, and covered with paraffin. The molds were then allowed to solidify at room temperature. Solid paraffin blocks were sectioned five microns thick and dried out overnight in a 40℃ incubator. Dried slides were then stored at -20℃ until stained.

Hematoxylin and Eosin Staining (H+E)

Slides prepared for H+E staining were baked at 60°C for one hour and then cooled to room temperature. Once cooled, the slides were placed in a staining tray and bathed in three consecutive xylene baths for three minutes each to remove the paraffin wax. To rehydrate the tissue, slides were bathed in two consecutive 100% ethanol baths for three minutes each, followed by two 95% ethanol baths, and finally a 70% ethanol bath, all three minutes each. Prior to staining, the slides were placed in distilled deionized water (DDi water) for five minutes in their staining tray. Finally, the slides were placed in a modified Harris hematoxylin for two minutes individually before being submerged in a flat dish of DDi water for 10 minutes. To decolorize the slides, they were removed from the water bath and tilted upright, allowing 0.25% 1N HCl diluted in pure ethanol to be gently pipetted onto the slides. The slides were then submerged again in a fresh, flat dish of DDi water for five minutes. Counterstaining was done by gently dipping the slides individually into Eosin Y for approximately 10 seconds. The slides were then loaded back into the staining tray and placed in a 70% ethanol bath for 3 minutes. To dehydrate the slides, the tray of slides was gently moved between two consecutive 95% ethanol baths, followed by two 100% ethanol baths, for three minutes each. Finally, slides were bathed in three consecutive xylene baths for three minutes each. Without letting the slides dry out, Cytoseal was applied to the front of the slide and a glass coverslip was placed on top to seal the stained tissues. Slides were then dried overnight before imaging.

Immunofluorescence Staining

Slides prepared for IF staining were first deparaffinized in three consecutive baths of xylene for three minutes each. The tissues were then rehydrated in two consecutive 100% ethanol baths, followed by two 95% ethanol baths, and finally a 70% ethanol bath, for three minutes each. While rehydrating, a staining dish was filled with 1x antigen retrieval buffer (Table 4) and microwaved to boil. The rehydrated slides were then placed in the boiling antigen retrieval buffer, covered to keep them from drying out, and simmered in the microwave for 20 minutes. Once cooled to room temperature, the slides were removed from the antigen retrieval buffer and a PAP pen was used to trace a circle of hydrophobic film around the tissue. Careful to not overflow the circled area of the slide containing the tissue, Superblock was pipetted onto the slides and allowed to incubate for one hour at room temperature. After incubation, the Superblock was removed from the slides and a cocktail of primary antibodies diluted 1:100 in Superblock was carefully pipetted onto their respective tissues. The primary antibodies used for the purposes of this thesis work are listed in Table 4. The primary antibodies were placed in a container on a bed of moist paper towels and incubated overnight at 4°C covered. The following day, the primary antibodies were removed from their respective tissues and the slides were placed in a dish of 1x phosphate buffered saline and 0.1% tween (PBS-T) and washed on a rocker for 10 minutes. After washing, a cocktail of secondary antibodies diluted 1:500 in Superblock was pipetted onto their respective tissues. The secondary antibodies used for the purposes of this thesis work are listed in Table 4. The secondary antibodies were incubated in a container at room temperature for one hour, and covered in tinfoil to keep the slides away from light. After incubation, the slides were washed once more in fresh PBS-T for 10 minutes, covered in tinfoil to keep the slides out of the light. After being washed, each slide was tilted upright and gently rinsed by pipetting 1x phosphate buffered saline onto the tissue. Finally, antifade with DAPI (Table 4) was applied to the slides and a glass coverslip was placed on top to seal the tissue. The slides were left to dry overnight in a cardboard slide folder to keep them in the dark.

Statistical Analysis

Data collected from the cells cultured to assess the effect of the small molecule inhibitors on growth were plotted in a scatter graph and then fitted with a logarithmic line of best fit. The coefficient of determination (R^2) is calculated to measure how reliable the line of best fit is to model the pattern of the plotted points; the closer the R^2 value is to one, the better the regression was at capturing the correlation between data points. The cell counts captured on the final day of the experiment were compared using a two-tailed t test of unequal variances, or Welch's t test. This test gives us a way to measure if the cell counts between our DMSO controls and our cells receiving treatments of our small molecule inhibitors are significantly different from one another. Welch's t test was also used to compare relative gene expressions for the qRT-PCR data.

RESULTS

5 uM doses of NOTCH1 small molecule inhibitors effectively inhibit NOTCH1 signaling

To establish the dose at which the cells would be cultured we utilized dosing from previously established studies, which used 10 uM for single treatments[36]. However, as the cells in our study will be cultured in a continuous exposure for 21+ days at the ALI, we also tested lower doses at 1 uM and 5 uM. Immortalized HBEC3-KT cells were cultured in monolayer for 7 days with continuous exposure to the SMI or DMSO control treatment, after which cells were harvested for qRT-PCR to establish the modulation of NOTCH pathway genes at each given dose. The results shown in Figure 7 of the qRT-PCR that revealed a significant difference in the downstream genes of *NOTCH1* including the expression of *HEY1* in 1 uM and 5 uM treatment concentrations when compared to the DMSO control cells. *HEY1* expression was significantly lower in NADI-351 (p=0.047), Crenigacestat (p=0.004), and DAPT (p=0.007) treated samples in the 1 uM doses. In the 5 uM treatment concentrations, *HEY1* was significantly lower (p=0.017) in DAPT treated cells. The cells treated with 5 uM DAPT also had a significantly lower expression of *HES2* (p=0.022). In the 10 uM doses there were no significant differences across any of the treatments of target genes. There was also no measurable expression of *HEYL* in the 10 uM treated cultures for any of the target genes.

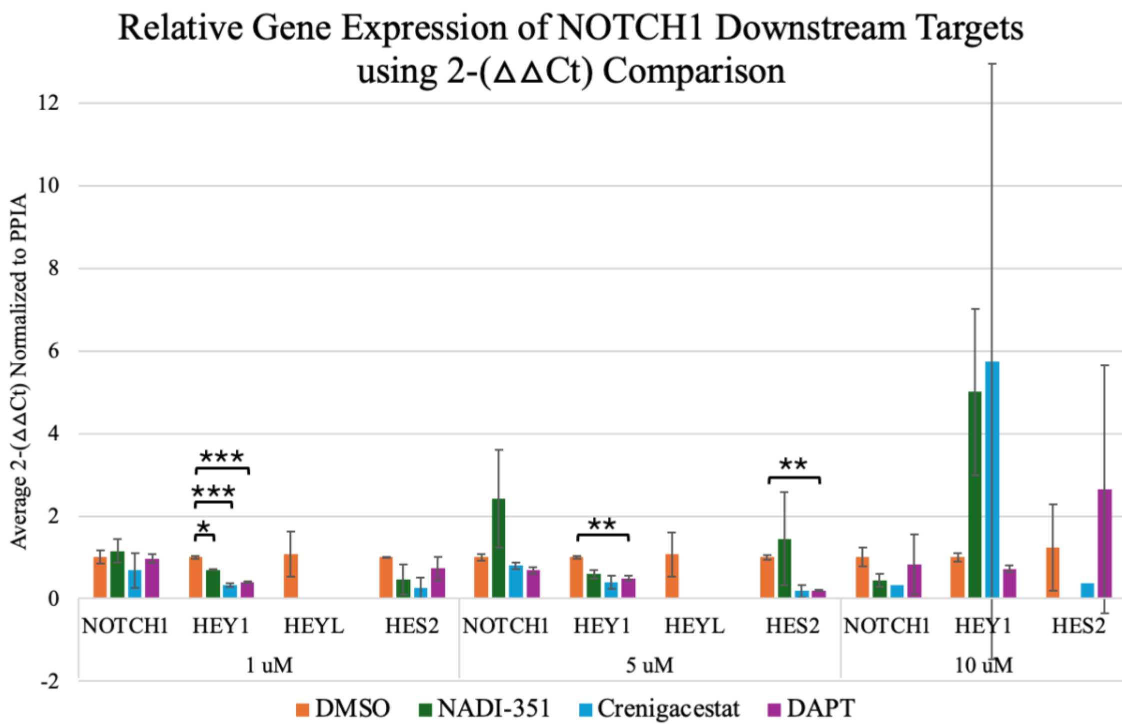

Figure 7. Gene expression of NOTCH1, HEY1, HEYL, and HES2 across treatments, measured by $2^{-\Delta\Delta CT}$ analysis. At 1 uM doses, significant differences were shown between controls and HEY1 in NADI-351, Crenigacestat, and DAPT (p=0.047, p=0.004, and p=0.007) treated cells. At 5 uM doses, significant differences were shown between controls and *HEY1* (p=0.017) and *HES2* (p=0.022) in DAPT treated cells. There were no significant differences amongst the cells treated with 10 uM doses of NOTCH1 SMI.

NOTCH1 inhibition by NADI-351 and DAPT suppress the growth of HBEC3-KT cells

To establish the effect of NOTCH1 inhibition on the growth of HBEC3-KT cells, HBEC3-KT cells were grown in monolayer culture for 2, 5, and 7 days. The cell number was enumerated to establish a growth curve (Figure 8). The cell counts taken on day seven were compared using a Welch's t test, to compare the number of cells grown after a 7 days of small molecule inhibitor treatments. There were no significant differences between the cell counts in our DMSO controls and the γ-secretase inhibitor Crenigacestat. Cell growth was significantly reduced in DAPT and NADI-351 treated HBEC3-KTs when compared to cell counts of the DMSO control cells (Figure 9).

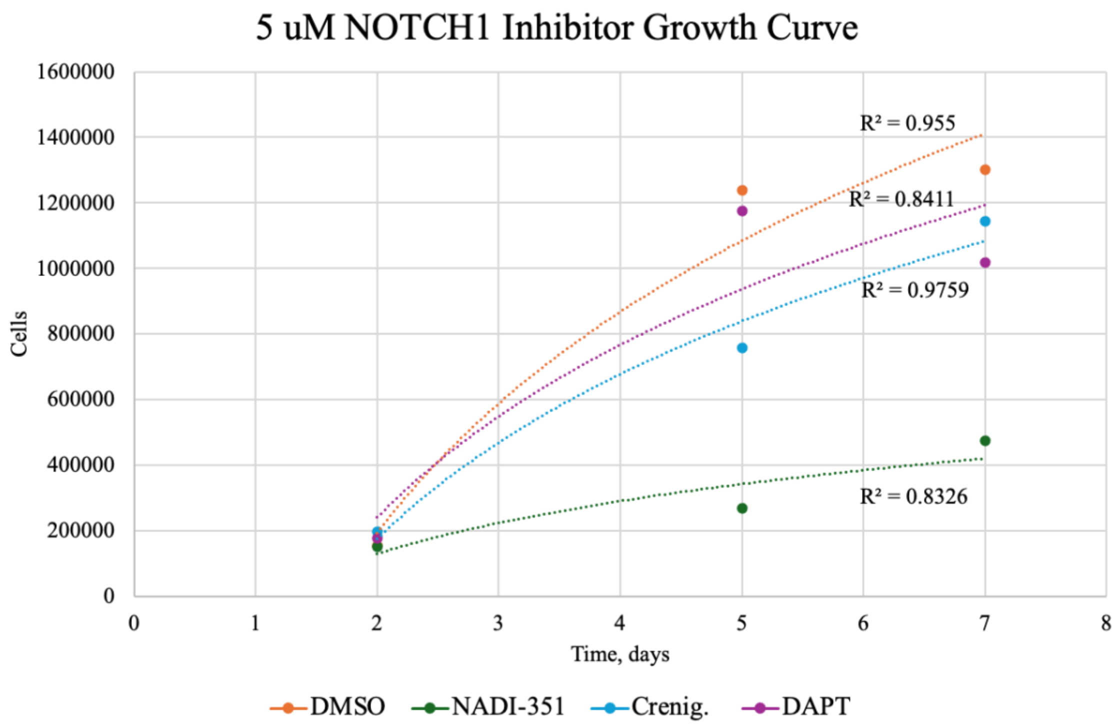

Figure 8. Average cell counts taken across each treatment for days two, five, and seven, fitted with logarithmic regression to chart trends in cell growth. Growth curves fitted to the DMSO and Crenigacestat data had the best correlation, though NADI-351 and DAPT still have values >0.80 which indicates that the data is still well represented by the curve.

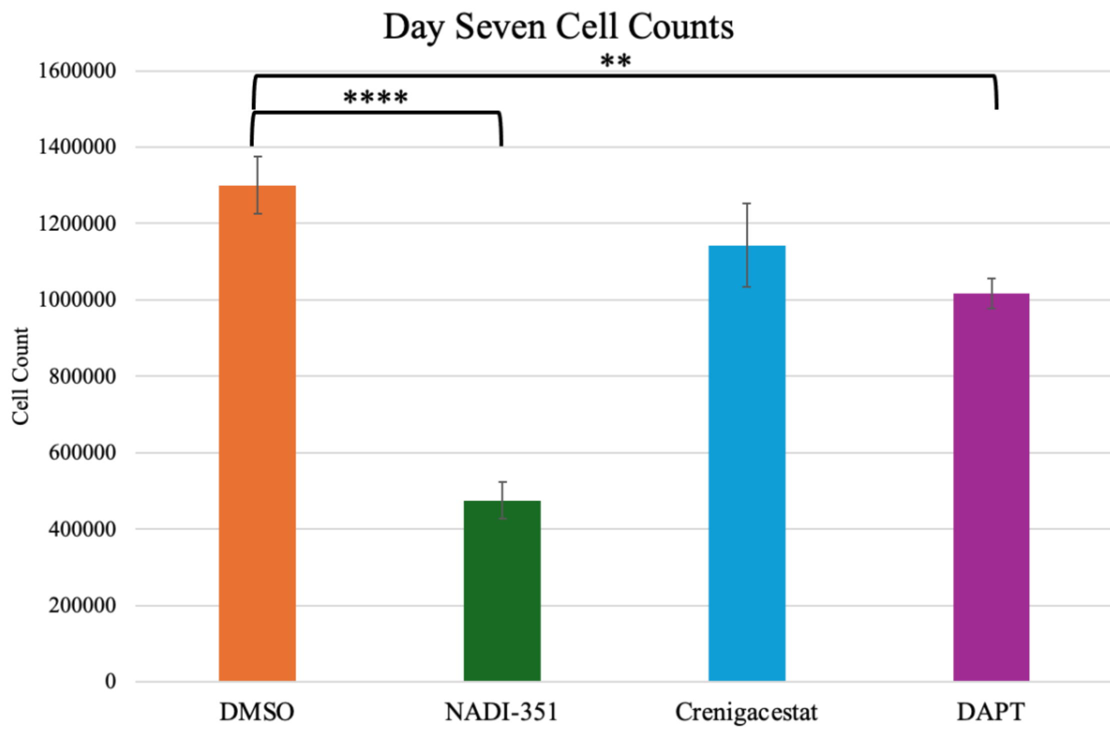

Figure 9. Cell counts taken on day seven for each NOTCH1 SMI treatment and controls. Cell counts were significantly lower in cultures treated with 5 uM NADI-351(p=0.0002) and DAPT (p=0.010) when compared to DMSO treated controls.

Primary HBEC Cells treated with 5 uM SMI lost cell adhesion but not due to apoptosis

Primary HBECs grown at the ALI were expanded and treated with 5 uM concentrations of NOTCH1 small molecule inhibitors. Shortly after starting small molecule inhibitor treatment, these cells began to separate from one another and had the appearance of blebbing around their edges. As blebbing is a sign of cell death like apoptosis the cells were harvested, once they had reached approximately 30%

confluence, and assessed for apoptotic markers[38]. Levels of NOTCH1 as well as three apoptotic markers were tested, *BAX*, *CASPASE-3*, and *BCL2* (Figure 10). These genes can be used as markers to determine if cells are apoptotic, with *BAX* and *CASPASE-3* being pro-apoptotic and *BCL2* being anti-apoptotic[39,40]. The expression of *BCL2* was not detected by qRT-PCR. However, there was no significant difference between the expression of the pro-apoptotic *BAX* and *CASPASE-3* in the inhibitor treatments compared to the DMSO control cells which were not observed to be dying. This shows that while these cells appeared to be undergoing a planned death, and has minor elevations in BAX, suggest apoptosis may not be the primary driver and more work is needed to establish the cause of loss of cell adhesion and blebbing.

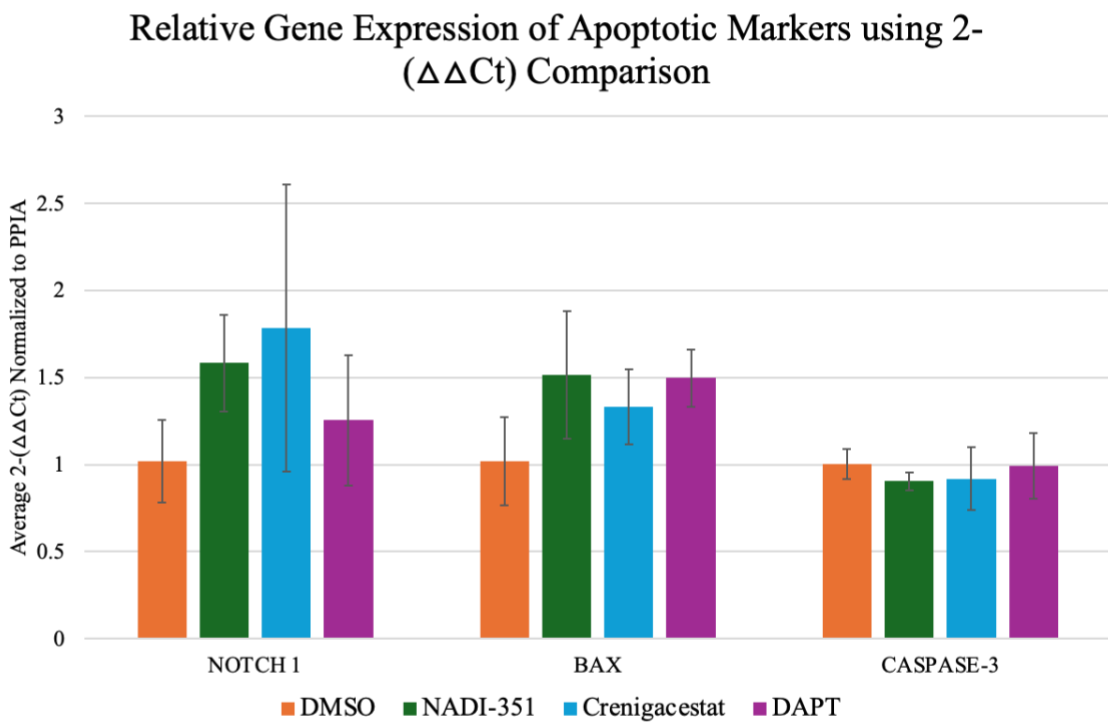

Figure 10. Relative gene expression of *NOTCH1*, and apoptotic markers *BAX* and *CASPASE-3* across treatments, measured by $2^{-\Delta\Delta CT}$ analysis. There are no significant differences across all treatments and genes.

Primary HBEC ALI treated with γ-secretase inhibitors have alterations in size and cell type distribution

To study changes in cell differentiation, while also avoiding the toxic effect of the higher 5 uM dose, we cultured pHBECs with 1 uM treatments of NOTCH1 SMI at the ALI. As previously described, these cells were grown out to confluence and then airlifted. Following airlift, the expansion media was replaced with maintenance media (Table 2) supplemented with 1 uM doses of NOTCH1 small molecule inhibitors. These cells were grown for 27 days post-airlift before being harvested for analysis.

We hypothesized that the inhibition of NOTCH1 would push the differentiation of primary HBEC cells towards a secretory lineage. To determine cell population shifts, samples were stained with H+E and IF. The H+E staining is used to visualize the tissues as a whole, allowing us to compare the thickness of the tissue, and visualize cell types with more distinct morphologies such as cilia or pockets of mucus (Figure 11). IF staining was used to stain specific proteins found in different cell lineages (Figure 12). Here we focused on antibodies specific for secretory lineages such as MUC5AC which is a protein associated with goblet cells, and CEACAM5 which is associated with the peri-goblet cell intermediate identified in previous studies[23]. Stains were also prepared for NOTCH1 to see the distribution of our inhibited target amongst our cells. Two additional stains were used as controls and to establish the orientation of the cells; DAPI, which stains the nuclei and is found in the mounting media used to produce these slides, and keratin 8, which is found in differentiated mature cells and is used to establish the orientation of the tissue. Unfortunately, the keratin 8 antibody stains were unable to be visualized with fluorescent microscopy.

All of the H+E images for the DMSO, NADI-351, and Crenigacestat cultures show an organized distribution of cells with cilia located along the apical surface of the tissue (Figure 11). The height of the DMSO control tissue is approximately 50 μm, which is roughly 3-4 layers of cells. The NADI-351 treated cells were visually similar to the DMSO control cells in terms of the H+E staining, with an even organization of cells and cilia. The thickness of the tissue cultured with NADI-351 treated media was also comparable to the DMSO controls, though slightly under 50 μm and only 2-3 layers of cells tall. Tissue collected from the Crenigacestat treated cultures showed some deviation in the appearance compared to the control tissue. The Crenigacestat treated tissue was thinner than the DMSO control cultures or NADI-351 cultures, and only approximately two layers of cells tall. The Crenigacestat treated tissue also had fewer cilia than the DMSO or NADI-351 treated cells. Imaging the DAPT treated cultures was quite difficult, as there was a loss of tissue during slide preparation. Slides were unable to be prepared for H+E staining, and the amount of tissue stained for IF was limited. While it was difficult to determine the total structure of the DAPT treated tissues, the size of the tissue visualized by IF would indicate that this culture was also thinner compared to the DMSO controls (Figure 12 and 13). No observations could be made about the presence and distribution of cilia using the IF images alone.

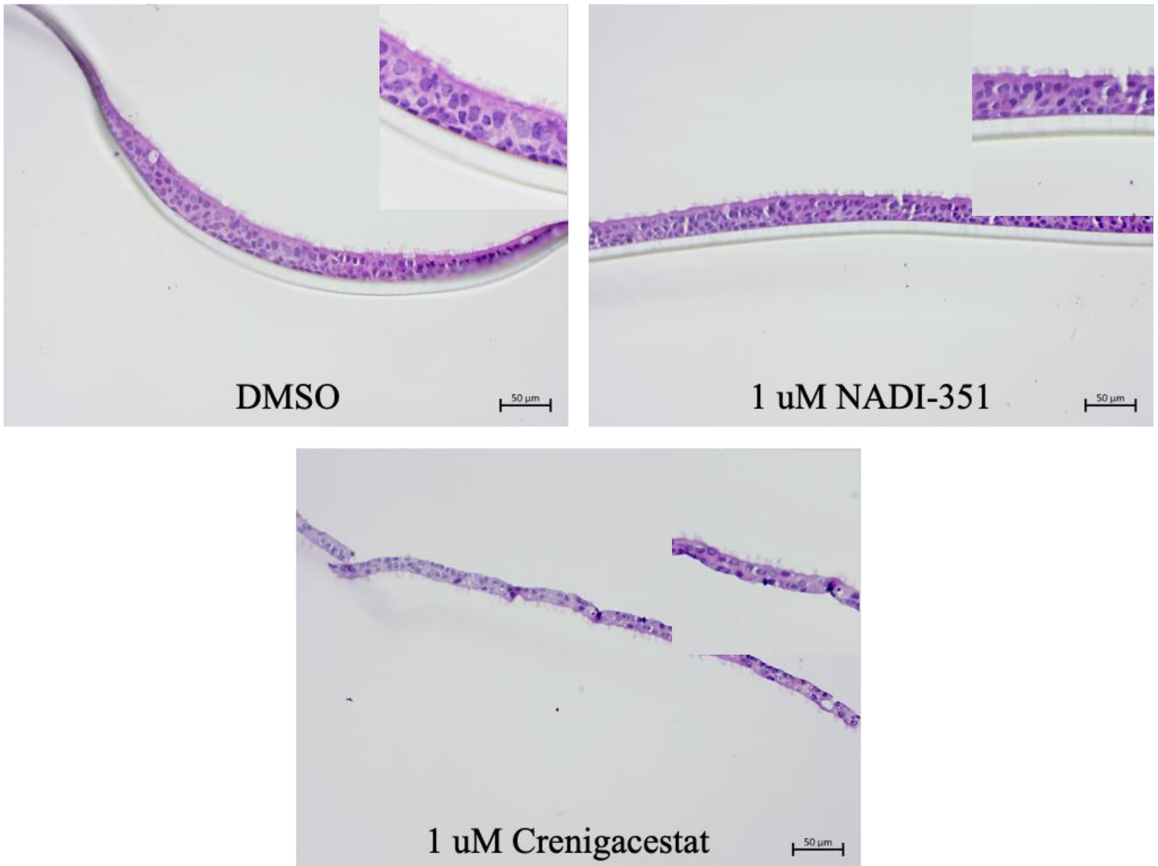

Figure 11. H+E staining of DMSO, NADI-351, and Crenigacestat ALI cultures. Cilia is present and evenly distributed in each sample, though the NADI-351 and Crenigacestat tissues were thinner than the DMSO control. The DMSO control tissue was roughly 3-4 cells tall, whereas the NADI-351 tissue was 2-3 cells tall, and the Crenigacestat tissue was 2 cells tall.

CEACAM5 expression was evenly expressed, though non-specific, across each SMI treatment. There were differences in the distribution of cells expressing MUC5AC between the control tissue and the two γ-secretase inhibitors Crenigacestat and DAPT. It can be seen from Figure 12 that MUC5AC expression, the goblet cell marker, is concentrated in pockets along the DMSO and NADI-351 tissue. These areas of concentrated fluorescence show that goblet cells are conservatively dispersed along the tissue. The Crenigacestat and DAPT treated cells show an increase in the distribution of MUC5AC expressing cells. Compared to the DMSO and NADI-351 treated cultures, the cells cultured with the two γ-secretase SMI show changes in cell fate that favor secretory goblet cells.

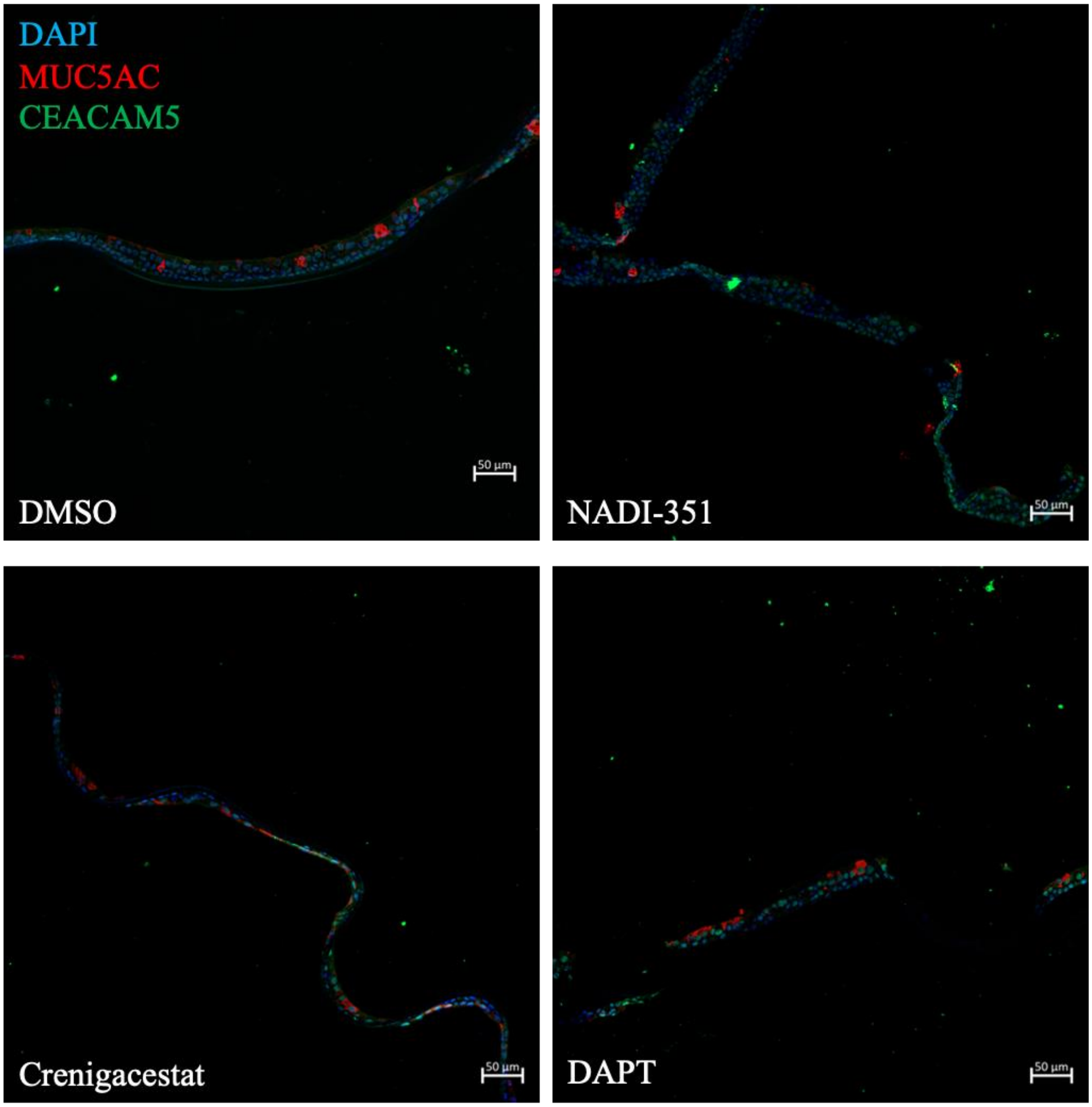

Figure 12. IF staining for DAPI, MUC5AC, and CEACAM5 in 1 uM NADI-351 treated primary HBEC cells cultured at the ALI for 27 days post-airlift. CEACAM5 expression is non-specific in each treatment. In the DMSO and NADI-351 treated cultures, there are pockets of MUC5AC-expressing goblet cells along the tissue. There is greater expression of MUC5AC in the Crenigacestat and DAPT treated tissues spread throughout the tissue.

There were no differences in the distribution of NOTCH1 any of the SMI treated cultures compared to the DMSO tissue. The staining for NOTCH1 and CEACAM5 were similar to each other, with the same non-specific staining along the tissue. However, NOTCH1 staining was primarily concentrated along both the apical and basal edges of the tissues.

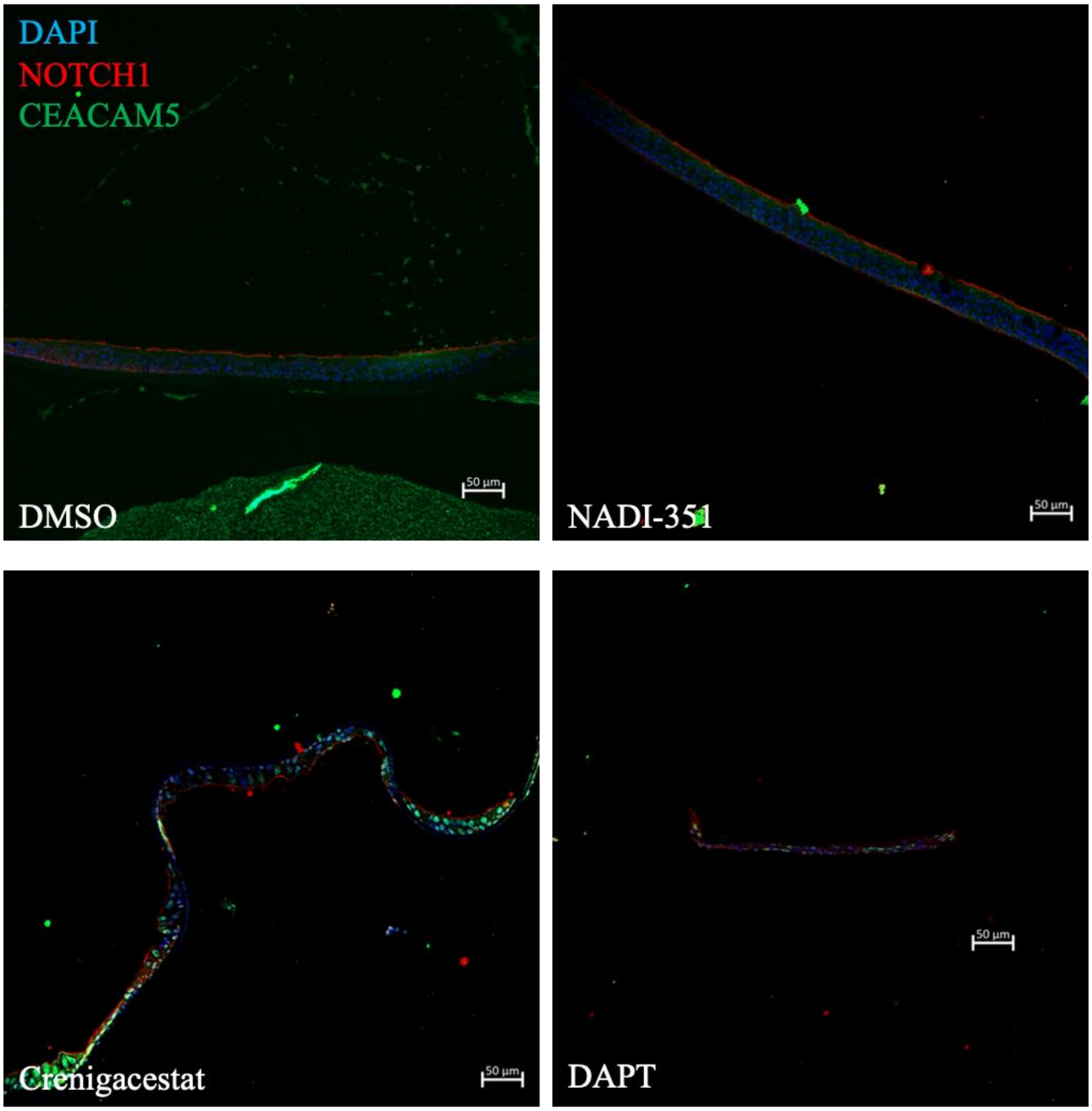

Figure 13. IF staining for DAPI, NOTCH1, and CEACAM5 in DMSO treated primary HBEC cells cultured at the ALI for 27 days post-airlift. Again, across each treatment there is non-specific staining of CEACAM5. NOTCH1 expression is limited to the outer edges of the tissue on both the apical and basal sides of the tissue.

DISCUSSION

Conclusions

The first aim of this study was to measure the effectiveness of NOTCH1 SMI, as well as establish the dosage sufficient for culturing HBECs by treating immortalized HBEC3-KTs with various doses of NOTCH1 SMI for 7 days, followed by qRT-PCR. Along with *NOTCH1*, three genes downstream of the NOTCH pathway (*HEY1, HEYL,* and *HES2)* were used to assess the effectiveness of the three SMI NADI-351, Crenigacestat, and DAPT. It was observed that 5 uM doses of *NOTCH1* SMI were most suitable for culturing, as the expression of genes downstream of NOTCH1 were still affected without completely losing expression of target genes like *HEYL*. The 10 uM treatment concentrations were deemed too high for culturing at the ALI because there were no significant differences between treatments or genes, and *HEYL* was unable to be detected even in the controls. This could be due to toxic effects of a continuous exposure at 10 uM rather than the one-time dose of 10 uM documented in the literature like with NADI-351[36].

Though not significant, there was an increase of *NOTCH1* expression in NADI-351 treated HBEC3-KTs across 1 uM and 5 uM treatment concentrations. This was unexpected, though this particular SMI has a different mechanism of action compared to the γ-secretase SMI DAPT and Crenigacestat. Rather than preventing the cleavage of NOTCH1, NADI-351 instead binds specifically to a pocket formed by the NOTCH intracellular domain and CSL protein, blocking Mastermind from binding and preventing the formation of the transcription complex[36]. The NOTCH pathway is able to regulate itself through feedback loops, which dictate when NOTCH signaling is turned "on" or "off" through lateral induction or inhibition based on the expression of molecules like NOTCH ligands, as well as which paths cells take during differentiation[41]. The successful cleavage of NOTCH1 at the membrane, but failed formation of the CSL transcription complex could be influencing the up regulation of NOTCH1. The expression of proteins downstream of NOTCH1 remain at low levels, which could be triggering the expression of NOTCH1 as a means to increase those protein levels. This would mean that the expression of targets like *HEY1* would still be low, but that *NOTCH1* would have an increase in expression compared to the controls.

The second aim of this study was to assess the effect of NOTCH1 SMI on the growth of HBEC3-KTs. As previously discussed, the effect of NOTCH1 inhibition on growth is typically dependent on the type of cell and the tissue microenvironment[29,30], so we wanted to establish the consequences of NOTCH1 inhibition specifically in HBEC3-KTs. After culturing with continuous NOTCH1 SMI for 7 days, we found that growth in the NADI-351 and DAPT treated cells was significantly inhibited compared to the controls. The growth of the Crenigacestat cells were not significantly inhibited, but the growth curve does suggest that there could be some inhibition of growth. This data supports the hypothesis that NOTCH1 inhibition would limit the growth of HBEC3-KTs.

These results were surprising since the Crenigacestat and DAPT SMI are both γ-secretase inhibitors, so it was expected that they would have had similar results. Instead, the more NOTCH-specific NADI-351 and DAPT had the significant inhibition of growth.

The experiment used to assess growth was a simple growth curve made by taking cell counts at various times throughout the 7 day treatment. While growth curves are reasonable methods for observing changes in growth between treatments of cell lines, they are not without their limitations. Losing cells during harvesting either during the spin down or resuspension, or the death of cells by trypsin exposure are all ways in which the cell count can be impacted by human error. Furthermore, automated cell counters are not infallible. Inadequate mixing before adding the cells to the disposable cell counting chambers can artificially inflate or deflate the counted number of cells, and if the focus of the camera within the cell counter is not properly set then some cells could be missed. In the future, differences in growth should be measured by metabolic assays like MTT assays or ATP assays. Both MTT and ATP assays measure cell viability through metabolic processes such as the conversion of MTT reagent to a color generating compound, or the binding of luciferin to ATP which is then catalyzed by luciferase to generate light[42]. These reactions can both be performed in a 96-well plate and be analyzed using a plate reader to measure absorbance.

The accompanying inhibition of cell growth in NOTCH1 SMI treated cells was not unexpected. One of the major roles that the NOTCH pathway fulfills is stem cell maintenance[26]. It is the NOTCH pathway which, during injury, triggers basal cells to grow and differentiate to repair tissue damages. If NOTCH is inhibited, it would be plausible that this process would also be hindered, stunting cell proliferation. In this way, perhaps the $NOTCH^{lof}$ found in bronchial biopsies of PML is actually protective in

LUSC, as it could be preventing the proliferation of cells which have been damaged by carcinogens and irritants.

The third and final aim of this thesis work was to establish changes in cell differentiation in primary HBEC cells treated with NOTCH1 SMI. Continuous exposure to 5 uM doses of SMI resulted in a loss of cells, particularly in the Crenigacestat and DAPT treated cultures, which appeared to be cell blebbing. To test if the toxicity of the 5 uM doses of SMI were resulting in apoptosis, the expression of apoptotic markers was measured using qRT-PCR. The expression of apoptotic markers *BAX* and *CASPASE-3*[39] was not significantly different across any of the treatments, suggesting that these cells were not apoptotic. The loss of cells could be an off-target effect of the SMI inducing a lack of adhesion between cells or between the cells and the transwell membrane, resulting in lifting. Previous study has shown that loss of NOTCH signaling destabilizes cell-cell adhesion in epithelial cells using both NOTCH knockout models and using the γ-secretase inhibitor DAPT[43]. The lifted cells could have then been cleaned away during routine PBS washes, which would give the appearance of cell death despite the cells simply separating from the membrane and each other. Seeing individual cells flake off from the edges of the tissue could also explain why the cells appear to be blebbing; instead of membrane protrusion what is actually observed is a cell lifting away from the membrane.

Cells grown at the ALI and treated with a reduced dose of 1 uM of the NOTCH1 SMI, successfully differentiated. There were very few differences in appearance between the NADI-351 treated cells and the DMSO controls, and when staining for IF the distribution of goblet cell markers (MUC5AC), peri-goblet cell markers (CEACAM5), and NOTCH1 there were no differences in expression. Only the physical size of the NADI-351 tissues were thinner than the controls. Expression of CEACAM5 was non-specific in all of the treatments, including the controls. Staining for NOTCH1 was concentrated on the outer luminal edge and basal layer in every treatment, indicating non-specificity. The non-specific staining of CEACAM5 and NOTCH1 was unexpected, and suggests that there is a problem with the staining or the specific antibodies used to stain. Because NOTCH1 is a membrane bound protein, it would be expected to be seen evenly distributed throughout the ALI tissues, not just along the outer edges. CEACAM5 as a peri-goblet cell marker would be expected to only appear in cells in the process of differentiating into goblet cells, so the even distribution of staining depicted here again suggests an issue with the antibody used or the staining technique.

Where the differences in differentiation were really seen was in the expression of MUC5AC, which is a goblet cell marker. DMSO controls and NADI-351 treated cells showed concentrated patches of MUC5AC expressing cells, indicating the presence of a goblet cell. These patches are evenly spaced, but not overwhelming the tissue, which we would expect since most of the bronchial epithelium should be made up of ciliated cells. The observed distribution of MUC5AC expressing goblet cells was as expected for normal, healthy airway tissue. In the two γ-secretase inhibitors, DAPT and Crenigacestat, not only were the tissues thinner than the controls, but MUC5AC expression was more distributed throughout the tissue suggesting that there were more goblet cells in these treatments.

As previously discussed, NADI-351 is more specific to the NOTCH pathway, as it inhibits specifically the formation for the CSL transcription factor. DAPT and Crenigacestat are less specific, and γ-secretase is used to cleave membrane bound proteins other than NOTCH. An inhibition of protein cleavage at the cell membrane, coupled with the inhibition of growth as demonstrated with our cell growth data and perhaps the loss of normal cell-cell would promote changes in the histology of tissues cultured with γ-secretase inhibitors.

Limitations

While the results of this thesis work are important for guiding the future of our study of NOTCH1 modulations in PML, there are limitations to the experiments presented here. The size of the study is our biggest limitation. A repetition of the dosage experiment should be performed again with an emphasis on culturing in triplicates or more. Two biological replicates is not sufficient to test for significance, though it works as a pilot to explore the most obvious differences between the 1 uM, 5 uM, and 10 uM doses of our SMI. Future experiments should incorporate more replicates, and should explore dosage with more granularity to optimize NOTCH1 inhibition while maintaining viability. Since 5 uM dose is too high for primary bronchial epithelial cells to grow at ALI, 5 uM can be used as the upper limit and doses between 1 uM and 5 uM can be incorporated. This would also establish the median lethal concentration, or the concentration at which half of our cells die. Establishing lethal doses is an important step in pharmaceutical development, and should further study reveal that NOTCH modulation could be a beneficial therapeutic for patients with PML, then that concentration will need to be established across cell lines, cell types, and organisms.

Aside from study size, there are improvements that can be made to some of the bench techniques that were employed here. For example, the cycle thresholds for the qRT-PCR data being in the 30s is relatively high, as these values typically sit around the low twenties. High cycle thresholds indicate that the starting quantity and/or quality of cDNA is low. During the RNA isolation process, impurities can be left behind such as salts from phenol-chloroform extraction or alcohols from RNA washing. These impurities are carried over to cDNA synthesis, which can prevent primers from binding and facilitating cDNA synthesis, contaminating the sample with unused dNTPs and synthesis materials, and falsely inflating NanoDrop quantification. This means that less of the target gene is actually in the sample being used for PCR. For example, using 40 ng of starting material that is contaminated could mean that only 10 ng of actual cDNA containing the target gene is present in the PCR reaction. This would increase the number of cycles it takes to amplify the targets, raising the Ct value. One way to circumvent this issue is to improve the techniques used in RNA isolation, like including additional wash steps and carefully removing only the aqueous layer during phenol-chloroform separation.

Another limitation of this thesis work, also pertaining to bench techniques, is the loss of tissue during staining. When processing and staining ALI samples it is possible to lose tissue, which occurred with the DAPT treated samples. ALI are very thin tissues, meaning there is less tissue present to adhere to the slide. The synthetic membrane also has a tendency to flake off of the slide, taking tissue with it in some instances. In the case of the DAPT treated cultures grown at the ALI, the tissue was likely so thin that very little was there to adhere to the slide, and what was there flaked off with the membrane during staining. To mitigate the loss of tissue, changes can be made to the staining protocol, including less abrasive washes, and subjecting the tissue to less physical trauma by being more gentle when moving between baths.

Future Directions

Goals for further study of the modulation of NOTCH1 in bronchial epithelium can be broken into short term and long term initiatives. In the short term, our focus is on validation of the data presented here. First and foremost, the study should be expanded to include more biological replicates. This gives more statistical power to the data and allows us to draw significant conclusions about the consequences of NOTCH1 modulation. Western blotting will also be employed to validate that the expression of proteins downstream of the NOTCH pathway are affected by the interruption of the pathway. While qPCR interrogates RNA levels, western blots would confirm the prescence or absence of proteins downstream of *NOTCH1* signaling. Finally, the use of more sensitive experiments, like the MTT or ATP assays, will be used to assess changes in cell growth when NOTCH1 is inhibited by SMI.

Aside from validation, more slides will be prepared to troubleshoot the loss of tissue in the DAPT treated ALI samples that occurred during staining, and more slides will be prepared for IF. Future IF stainings should make use of antibodies specific to ciliated populations such as acetylated α-tubulin or FOXJ1, which is a transcription factor involved in cilia production. A second staining for CEACAM5 and NOTCH1 is also necessary to troubleshoot the lack of cell-specific staining. Special care should be taken when washing the slides following antibody incubation, and different antibody clones should be considered.

Long term goals for this project, which are already underway by other researchers in our group, focus less on how NOTCH1 modulation affects healthy HBECs, but on building an *in vitro* model of PML morphologies typically seen in patient biopsies. Culturing primary HBECs with inflammatory molecules like interleukin 13 and irritants like cigarette smoke condensate have already successfully stimulated goblet cell hyperplasia in primary HBECs grown at ALI[21]. In the future we would like to study the effect of $NOTCH1^{lof}$ cells when co-cultured with healthy cells and treated with inflammatory molecules like the interleukins or cigarette smoke condensate. This project involves a knockout or mutation of *NOTCH* in cells, along with the addition of a fluorescent tag to help identify which cells are $NOTCH^{lof}$ cells.

The continuation of this project, both short term and long term, centers on understanding the role NOTCH plays in the progression or regression of PML, and determining if NOTCH1 is a driver or protector during PML development. This understanding will not only help us better identify aggressive lesions in patients, but could also provide us with opportunities to develop therapeutics targeted at PML. By identifying these lesions early, before the point of becoming established cancer, we hypothesize that patient survival will improve and that the burden of lung cancer can be ameliorated.

BIBLIOGRAPHY

1. Common Cancer Sites - Cancer Stat Facts. *SEER* https://seer.cancer.gov/statfacts/html/common.html.

2. Types of Lung Cancer. *American Lung Association* https://www.lung.org/lung-health-diseases/lung-disease-lookup/lung-cancer/basics/lung-cancer-types (2023).

3. What Is Lung Cancer? | Types of Lung Cancer. https://www.cancer.org/cancer/types/lung-cancer/about/what-is.html.

4. Sabbula, B. R., Gasalberti, D. P. & Anjum, F. Squamous Cell Lung Cancer. in *StatPearls* (StatPearls Publishing, Treasure Island (FL), 2024).

5. Kawase, A. *et al.* Differences Between Squamous Cell Carcinoma and Adenocarcinoma of the Lung: Are Adenocarcinoma and Squamous Cell Carcinoma Prognostically Equal? *Japanese Journal of Clinical Oncology* **42**, 189–195 (2012).

6. Wang, W., Liu, H. & Li, G. What's the difference between lung adenocarcinoma and lung squamous cell carcinoma? Evidence from a retrospective analysis in a cohort of Chinese patients. *Frontiers in Endocrinoogy.* **13**, 947443 (2022).

7. How Is Lung Cancer Diagnosed? *American Lung Association* https://www.lung.org/lung-health-diseases/lung-disease-lookup/lung-cancer/symptoms-diagnosis/how-is-lung-cancer-diagnosed.

8. Spira, A. *et al.* Airway epithelial gene expression in the diagnostic evaluation of smokers with suspect lung cancer. *Nature Medicine* **13**, 361–366 (2007).

9. Perez-Rogers, J. F. *et al.* Shared Gene Expression Alterations in Nasal and Bronchial Epithelium for Lung Cancer Detection. *Journal of the National Cancer Institute* **109**, djw327 (2017).

10. Cancer Staging: What Stages & Grades Mean. *Cleveland Clinic* https://my.clevelandclinic.org/health/diagnostics/22607-cancer-stages-grades-system.

11. Woodard, G. A., Jones, K. D. & Jablons, D. M. Lung Cancer Staging and Prognosis. in *Lung Cancer: Treatment and Research* (ed. Reckamp, K. L.) 47–75 (Springer International Publishing, Cham, 2016). doi:10.1007/978-3-319-40389-2_3.

12. Chang, J. T.-H., Lee, Y.-M. & Huang, R. S. The Impact of the Cancer Genome Atlas on Lung Cancer. *Translation Research* **166**, 568 (2015).

13. The Cancer Genome Atlas Program (TCGA) - NCI. https://www.cancer.gov/ccg/research/genome-sequencing/tcga (2022).

14. Wacholder, S. Precursors in Cancer Epidemiology: Aligning Definition and Function. *Cancer Epidemiology Biomarkers & Prevention* **22**, 521–527 (2013).

15. Ishizumi, T., McWilliams, A., MacAulay, C., Gazdar, A. & Lam, S. Natural history of bronchial preinvasive lesions. *Cancer Metastasis Reviews* **29**, 5–14 (2010).

16. Teixeira, V. H. *et al.* Deciphering the genomic, epigenomic, and transcriptomic landscapes of pre-invasive lung cancer lesions. *Nature Medicine* **25**, 517–525 (2019).

17. Breuer, R. H. *et al.* The Natural Course of Preneoplastic Lesions in Bronchial Epithelium. *Clinical Cancer Research* **11**, 537–543 (2005).

18. Campbell, J. D. *et al.* The Case for a Pre-Cancer Genome Atlas (PCGA) | Cancer Prevention Research | American Association for Cancer Research. https://aacrjournals.org/cancerpreventionresearch/article/9/2/119/50506/The-Case-for-a-Pre-Cancer-Genome-Atlas-PCGA-The.

19. Beane, J. *et al.* Detecting the Presence and Progression of Premalignant Lung Lesions via Airway Gene Expression. *Clinical Cancer Research* **23**, 5091–5100 (2017).

20. Beane, J. E. *et al.* Molecular subtyping reveals immune alterations associated with progression of bronchial premalignant lesions. *Nature Communications* **10**, 1856 (2019).

21. Pfefferkorn, R. M. *et al.* Abstract PR004: The role of NOTCH1 in bronchial pre-malignant lesions. *Cancer Prevention Research (Phila. Pa.)* **16**, PR004 (2023).

22. Bustamante-Marin, X. M. & Ostrowski, L. E. Cilia and Mucociliary Clearance. *Cold Spring Harbor Perspectives in Biology* **9**, a028241 (2017).

23. Characterizing smoking-induced transcriptional heterogeneity in the human bronchial epithelium at single-cell resolution. *Science Adv* (2019) doi:10.1126/sciadv.aaw3413

24. Fiúza, U.-M. & Arias, A. M. Cell and molecular biology of Notch. *Journal of Endocrinology* **194**, 459–474.

25. Kopan, R. & Ilagan, Ma. X. G. The Canonical Notch Signaling Pathway: Unfolding the Activation Mechanism. *Cell* **137**, 216–233 (2009).

26. Rock, J. R. *et al.* Notch-dependent differentiation of adult airway basal stem cells. *Cell Stem Cell* **8**, 639–648 (2011).

27. Li, J., Li, H., Zhang, C., Zhang, C. & Wang, H. Integrative analysis of genomic alteration, immune cells infiltration and prognosis of lung squamous cell carcinoma (LUSC) to identify smoking-related biomarkers. *International Immunopharmacology* **89**, 107053 (2020).

28. Cumplido-Laso, G., Benitez, D. A., Mulero-Navarro, S. & Carvajal-Gonzalez, J. M. Transcriptional Regulation of Airway Epithelial Cell Differentiation: Insights into the Notch Pathway and Beyond. *International Journal of Molecular Sciences* **24**, 14789 (2023).

29. Westhoff, B. *et al.* Alterations of the Notch pathway in lung cancer. *Proceedings of the National Academy of Sciences* **106**, 22293–22298 (2009).

30. Zheng, Q. *et al.* Notch signaling inhibits growth of the human lung adenocarcinoma cell line A549. *Oncology Reports* **17**, 847–852 (2007).

31. Fleming, R. J. Structural conservation of Notch receptors and ligands. *Seminars in Cell and Developmental Biology* **9**, 599–607 (1998).

32. Kunze, B. *et al.* Notch signaling drives development of Barrett's metaplasia from Dclk1-positive epithelial tuft cells in the murine gastric mucosa. *Scientific Reports* **11**, 4509 (2021).

33. van Es, J. H. *et al.* Notch/gamma-secretase inhibition turns proliferative cells in intestinal crypts and adenomas into goblet cells. *Nature* **435**, 959–963 (2005).

34. Dong, Z. *et al.* Gamma-Secretase Inhibitor (DAPT), a potential therapeutic target drug, caused neurotoxicity in planarian regeneration by inhibiting Notch signaling pathway. *Science of the Total Environment* **781**, 146735 (2021).

35. Mancarella, S. *et al.* Crenigacestat, a selective NOTCH1 inhibitor, reduces intrahepatic cholangiocarcinoma progression by blocking VEGFA/DLL4/MMP13 axis. *Cell Death and Differentiation* **27**, 2330–2343 (2020).

36. Alvarez-Trotta, A. *et al.* Pharmacological disruption of the Notch1 transcriptional complex inhibits tumor growth by selectively targeting cancer stem cells. *Cancer Research* **81**, 3347–3357 (2021).

37. Pfaffl, M. W. Quantification strategies in real-time PCR. in *A-Z of quantitative PCR* 87–112 (International University Line, La Jolla, CA, 2004).

38. Barros, L. F. *et al.* Apoptotic and necrotic blebs in epithelial cells display similar neck diameters but different kinase dependency. *Cell Death and Differentiation* **10**, 687–697 (2003).

39. Kapoor, E. *et al.* Expression Profile of Markers of Apoptosis, Injury and Oxidative Stress in Human Lung Epithelium Cells-A5449 Receiving Chronic Exposure of Potential Anti-Tubercular Drug-trans-Cyclohexane-1, 4-Diamine Derivative-“9u”. *Toxicology International* **21**, 172–178 (2014).

40. Tesfaigzi, Y. Roles of Apoptosis in Airway Epithelia. *American Journal of Respiratory Cell and Molecular Biology* **34**, 537–547 (2006).

41. Sjöqvist, M. & Andersson, E. R. Do as I say, Not(ch) as I do: Lateral control of cell fate. *Developmental Biology* **447**, 58–70 (2019).

42. Riss, T. L. *et al.* Cell Viability Assays. in *Assay Guidance Manual* (eds. Markossian, S. et al.) (Eli Lilly & Company and the National Center for Advancing Translational Sciences, Bethesda (MD), 2004).

43. White, M. J., Jacobs, K. A., Singh, T. & Kutys, M. L. Notch1 cortical signaling regulates epithelial architecture and cell-cell adhesion. *bioRxiv* 2023.01.23.524428 (2023) doi:10.1101/2023.01.23.524428.

CURRICULUM VITAE

[redacted]

[redacted]